STRESS CONCENTRATION FACTORS AROUND A CIRCULAR HOLE IN LAMINATED COMPOSITES

C. E. S. Ueng
Georgia Institute of Technology

SUMMARY

This paper deals with the determination of stress concentration factors around a circular hole in a composite laminate. The specific case investigated is a four layer ($-45^o/45^o/45^o/-45^o$) graphite epoxy laminate. The factors are determined experimentally by means of electrical resistance strain gages, and analytically by using a hybrid finite-element analysis.

INTRODUCTION

In this study, the laminar stress concentrations around a circular hole in an angle-ply composite laminate are determined for the axial tension loading case. Of particular interest is the largest value of σ_θ present at the perimeter of the hole. This study proposes to determine these stresses experimentally and analytically. For the experimental analysis, electrical resistance strain gages are used. The analytic procedure uses the finite-element method of a two-dimensional hybrid model with an assumed stress field within the element and assumed displacements at the element interfaces.

The stress concentration factors around a circular hole in an infinite, isotropic sheet have been determined analytically through various approaches and confirmed experimentally. For an infinite plate, the stress components around the hole are (ref. 1)

$$\sigma_r = \frac{\sigma_o}{2}\left(1 - \frac{b^2}{r^2}\right) + \frac{\sigma_o}{2}\left(1 - \frac{b^2}{r^2}\right)\left(1 - \frac{3b^2}{r^2}\right)\cos 2\theta \tag{1a}$$

$$\sigma_\theta = \frac{\sigma_o}{2}\left(1 + \frac{b^2}{r^2}\right) - \frac{\sigma_o}{2}\left(1 + \frac{3b^4}{r^4}\right)\cos 2\theta \tag{1b}$$

$$\tau_{r\theta} = -\frac{\sigma_o}{2}\left(1 - \frac{b^2}{r^2}\right)\left(1 + \frac{3b^2}{r^2}\right)\sin 2\theta \tag{1c}$$

where b is the radius of the hole and σ_o is the applied load. The ratio of σ_θ/σ_o along the hole is plotted as shown in figure 1. Obviously, the maximum

of σ_θ is three times σ_o, and occurs at $\theta = \pm 90^o$, i.e., at the ends of the diameter perpendicular to the direction of tension.

Due to the increasing use of advanced laminated composites in flight structures and other potential applications, the stress concentration around a cutout in a fiber-reinforced laminate has been the subject of research by several investigators in recent years. Daniel and Rowland (ref. 2) used an experimental approach - the Moire technique, and determined the strain (stress) concentration around a circular hole in a tension loaded anisotropic plate. Hyman et al. (ref. 3) carried some exploratory tests on the same problem. Franklin (ref. 4) also investigated the hole stress concentrations in filamentary structures. By using linear elastic plane stress conditions with the help of finite-element method, Rybicki and Hooper (ref. 5) studied and obtained results for boron-epoxy lamina. In a reviewing article (ref. 6), Grimes and Greimann gave an up-to-date overall picture about the stress concentration around a circular hole in a fiber-reinforced composite. Several additional references are cited in this article.

In an experimental study of orthotropic composite materials, Kulkarni, Rosen, and Zweben (ref. 7) have found that the stress concentration factors are a function of the hole diameter, up to a diameter of 2.54 cm (1 in.). They observed that the actual number of filaments severed by the hole determined the strength of the specimen.

The present problem of a general angle-ply composite laminate with a circular hole is further complicated by the interaction of the individual layers.

EXPERIMENTAL WORK

Equipment

The orientation of the strain gages around the holes is shown for each of the four specimens in figure 2. The gages were mounted adjacent to the hole and were 4.8 mm (3/16 in.) wide, 120 ohm standard foil gages. The specimens were mounted in clamp grips and attached to a 90,000 N (20,000 lb.) capacity load cell through the use of swivel bearings. The gages were wired into the digital strain indicator with the indicator providing three arms of the Wheatstone bridge required in the electrical circuit. The load cell was wired into an electrical transducer and calibrated to measure the axial tension applied to the specimens.

The strain gages were applied to the specimens using Eastman 910 adhesive, following standard preparation of the surfaces.

Test Specimen Data

The four testing specimens were provided by Lockheed-Georgia Aircraft Company. Their assistance is greatly appreciated.

Material: graphite epoxy (Narmco 5209/T300)

65% graphite fiber, 35% epoxy matrix

Four layer angle-ply ($-45^{o}/45^{o}/45^{o}-45^{o}$)

Grip tabs of fiberglass epoxy molded integrally with specimens.

For a unidirectional single layer the macroscopic properties are

$$E_{0^o} = 137900 \sim 144795 \text{ MN/m}^2 \ (20 \sim 21(10)^6 \text{ psi})$$

$$E_{90^o} = 8274 \sim 9653 \text{ MN/m}^2 \ (1.2 \sim 1.4(10)^6 \text{ psi})$$

$$G = 4.55 \text{ MN/m}^2 \ (0.66(10)^6 \text{ psi})$$

Specimen No.	1	2	3	4
Width	10.16 cm (4 in)	10.16 cm (4 in)	10.16 cm (4 in)	10.16 cm (4 in)
Hole diameter	2.5522 cm (1.0048 in)	2.5527 cm (1.0050 in)	2.5527 cm (1.0050 in)	2.5530 cm (1.0051in)

The thickness of the four specimens around the hole was also carefully measured. Data were taken at eight stations, the end points of a horizontal diameter, a vertical diameter, and two more diameters which bisect the horizontal and vertical directions. The results are shown in table 1.

It can therefore be concluded that the assumed thickness 0.6350 mm (0.0250 in) is quite reasonable.

Testing Procedure

First, the testing specimen was mounted in the upper grips of the loading device. The loading indicator and the strain indicator were zeroed and calibrated. Then the other end of the specimen was mounted in the lower grips of the loading device. After the specimen was loaded up to the 100% load (2224 N or 500 lb), the load was then released. This was repeated six times in order to eliminate the strain gage error due to strain hardening. An increment of 20% of the maximum load was used each time, and the corresponding strain reading was then taken. The same steps were followed for the other three specimens.

Testing Results

The data obtained from the strain gage testing was the values for ϵ_θ at

four different locations around the hole. These values are given in table 2, and displayed graphically in figure 3.

The strain gage results can be easily repeated and showed very good stability with repeated loadings. The values obtained at 444.8 N (100 lb) of load are not as reliable as the incremental changes in strain for each incremental change in load. Normally, the tightening of the end clamps on the specimens resulted in an initial strain of some significance.

The assistance of Mr. W. H. Taylor in carrying out the testing program is acknowledged here.

Stresses

Based upon the available mechanical properties as previously mentioned, the stresses were calculated from the stress-strain relation and the transformation relations. The tangential stress component σ_θ obtained from the recorded strains are plotted in figure 4.

FINITE ELEMENT ANALYSIS

The finite-element method used here is a two-dimensional hybrid approach. The variational principle used is that of minimum complementary energy with the interelement stress continuity enforced by means of the Lagrange multipliers. The elements used are shown in figure 5.

The formulation of the problem at this stage follows a rather standard fashion as this method is typically applied to many stress analysis problems.

The stress function polynomial used in the computer program is

$$\psi = ax^3 + bx^2y + cxy^2 + dy^3 \tag{2}$$

which results in the following stresses:

$$\begin{aligned} \sigma_{xx} &= 2\,cx + 6\,dy \\ \sigma_{yy} &= 6\,ax + 2\,by \\ \tau_{xy} &= -2\,bx - 2\,cy \end{aligned} \tag{3}$$

It can be easily verified that these stress components automatically satisfy the equilibrium equations in the absence of body forces.

Arranged in matrix form, equations (3) become

$$[\sigma] = [Q]\,[a] \tag{4}$$

where

$$[Q] = \begin{bmatrix} 0 & 0 & 2x & 6y \\ 6x & 2y & 0 & 0 \\ 0 & -2x & -2y & 0 \end{bmatrix} \quad \text{and} \quad [a] = \begin{bmatrix} a \\ b \\ c \\ d \end{bmatrix}$$

By Cauchy's relation $T_i = \sigma_{ij} n_j$, one has

$$\begin{matrix} T_x \\ T_y \end{matrix} = \begin{bmatrix} n_x & 0 & n_y \\ 0 & n_y & n_x \end{bmatrix} \begin{bmatrix} \sigma_{xx} \\ \sigma_{yy} \\ \tau_{xy} \end{bmatrix} \tag{5}$$

or

$$[T] = [M]\,[a] \tag{6}$$

where

$$[M] = \begin{bmatrix} n_x & 0 & n_y \\ 0 & n_y & n_x \end{bmatrix} [Q] \tag{7}$$

Following a somewhat standard fashion, the circumferential stress around the hole is obtained and plotted also in figure 4 for the comparison purpose.

DISCUSSION OF RESULTS

The results presented in this paper represent an attempt to understand and predict the stress concentration around a circular hole in an angle-ply laminate. As shown in figure 4, the circumferential stresses, based upon the finite-element method and the one computed from the recorded strain data, are plotted together for comparison purpose. These two curves cross each other at a few places, but the discrepancy at some places is up to 35%. This degree of deviation is not hoped for, but it is tolerable. Similar experience indicates that such a difference is by all means possible.

The stress concentration factor at $b/r = 1$ and $\theta = \pm 90^\circ$ is about 5.8

which is considerably higher than the classical factor 3 for an infinite, isotropic plate. Therefore, special attention must be paid for the local stress concentration around such a circular hole. One possible reason for having such a high stress concentration factor is that a number of fibers were cut at the location of the hole. This weakens the ability of the fiber elements for transmitting the stresses. From an intuitive point of view, if the location of the hole is known in advance, then rerouting the fibers around the hole may cut down the high stress concentration factor.

REFERENCES

1. Timoshenko, S. P. and Goodier, J. N.: Theory of Elasticity, Third Edition, McGraw-Hill, 1970, p. 91.

2. Daniel, I. M. and Rowland, R. E.: Determination of Strain Concentration in Composites by Moiré Techniques, Journal of Composite Materials, vol. 5, April 1971, pp. 250-254.

3. Hyman, B. I., DeTurk, A., Diaz, R., and DiGiovanni, G.: Exploratory Tests on Fiber-Reinforced Plates with Circular Holes Under Tension, AIAA Journal, vol. 7, no. 9, September 1969, pp. 1820-1821.

4. Franklin, H. G.: Hole Stress Concentrations in Filamentary Structures, Fibre Science and Technology, vol. 2, 1970.

5. Rybicki, E. F., and Hooper, A. T.: Analytical Investigation of Stress Concentrations Due to Holes in Fiber Reinforced Plastic Laminated Plates, Two-Dimensional Models, AFML-TR-72-15, U.S. Air Force, 1972.

6. Grimes, G. C. and Greimann, L. F.: Analysis of Discontinuities, Edge Effects, and Joints, Chapter 10, vol. 8, Structural Design and Analysis, Part II, edited by C. C. Chamis, in Composite Materials, Academic Press, 1974.

7. Kulkarni, S. V., Rosen, B. W., and Zweben, C.: Load Concentration Factors for Circular Holes in Composite Laminates, Journal of Composite Materials, vol. 7, July 1973, pp. 387-393.

TABLE 1.- TEST SPECIMEN DATA

Station	Thickness, mm (in.) for specimen —			
	1	2	3	4
0^{o}	0.5842 (0.0230)	0.6477 (0.0255)	0.6223 (0.0245)	0.5969 (0.0235)
45^{o}	0.5969 (0.0235)	0.6477 (0.0255)	0.6350 (0.0250)	0.5842 (0.0230)
90^{o}	0.6477 (0.0255)	0.6350 (0.0250)	0.6350 (0.0250)	0.5842 (0.0230)
135^{o}	0.6731 (0.0265)	0.6604 (0.0260)	0.6096 (0.0240)	0.5842 (0.0230)
180^{o}	0.6477 (0.0255)	0.6731 (0.0265)	0.6350 (0.0250)	0.5969 (0.0235)
-135^{o}	0.6223 (0.0245)	0.6731 (0.0265)	0.6350 (0.0250)	0.5969 (0.0235)
-90^{o}	0.5969 (0.0235)	0.6350 (0.0250)	0.6477 (0.0255)	0.5969 (0.0235)
-45^{o}	0.5842 (0.0230)	0.6477 (0.0255)	0.6223 (0.0245)	0.6223 (0.0245)

TABLE 2.- TEST RESULTS

Applied load, N (lb)	Remote stress, kN/m^2 (ksi)	Strain recorded, mm/mm or in./in., for specimen —			
		1	2	3	4
448.8 (100)	6895 (1)	1520×10^{6}	-990×10^{6}	390×10^{6}	108×10^{6}
889.6 (200)	13790 (2)	2610×10^{6}	-1710×10^{6}	600×10^{6}	250×10^{6}
1334.4 (300)	20685 (3)	3730×10^{6}	-2690×10^{6}	830×10^{6}	398×10^{6}
1779.2 (400)	27580 (4)	4920×10^{6}	-3540×10^{6}	1020×10^{6}	551×10^{6}
2224 (500)	34475 (4)	6170×10^{6}	-4600×10^{6}	1230×10^{6}	710×10^{6}

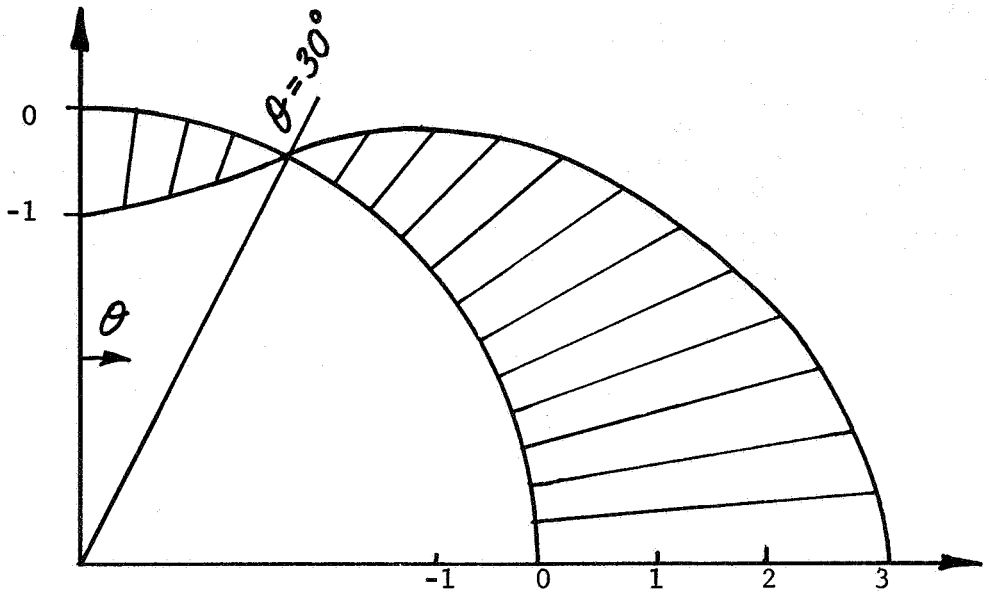

Figure 1.- Isotropic case, σ_θ/σ_o.

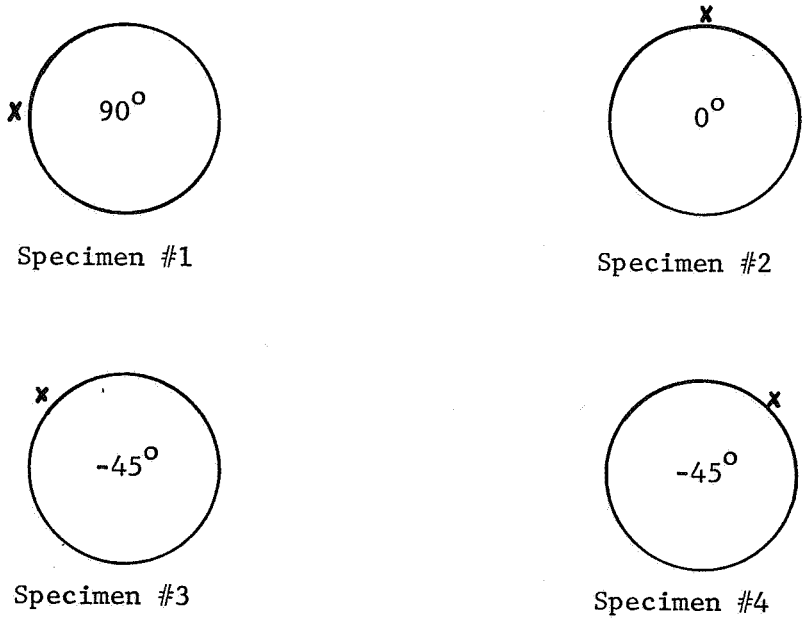

Figure 2.- Location of strain gages.

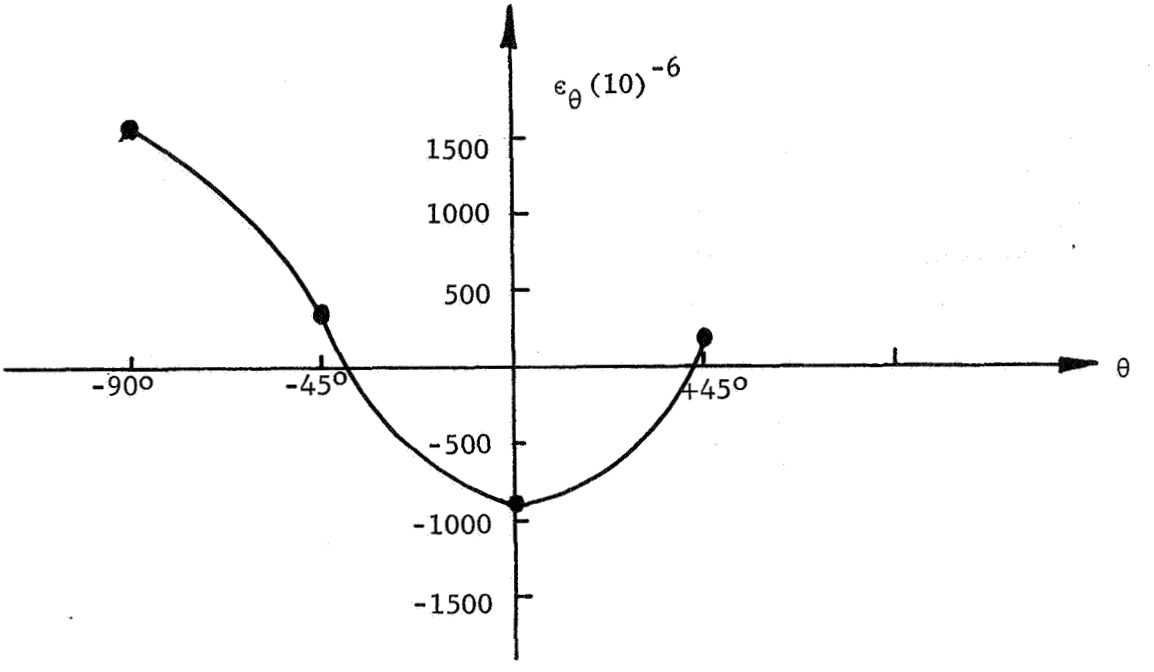

Figure 3.- Strain curve, σ_o = 6895 kN/m^2 (1 ksi).

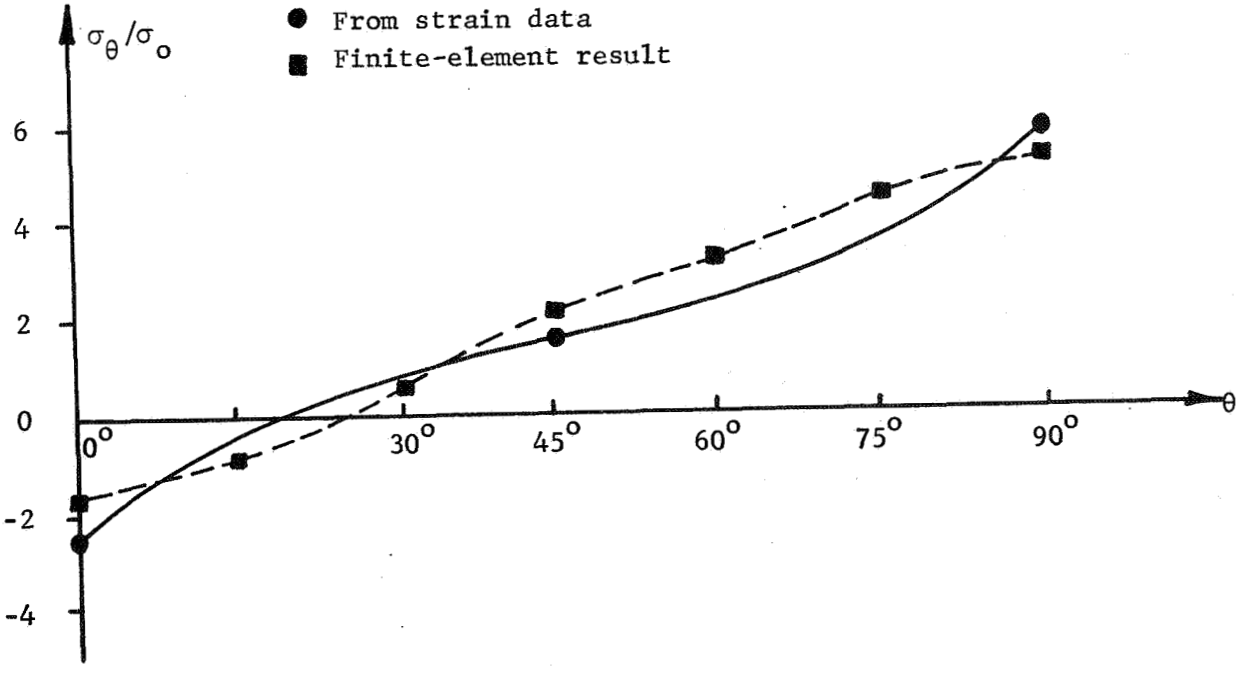

Figure 4.- Stress concentration factors.

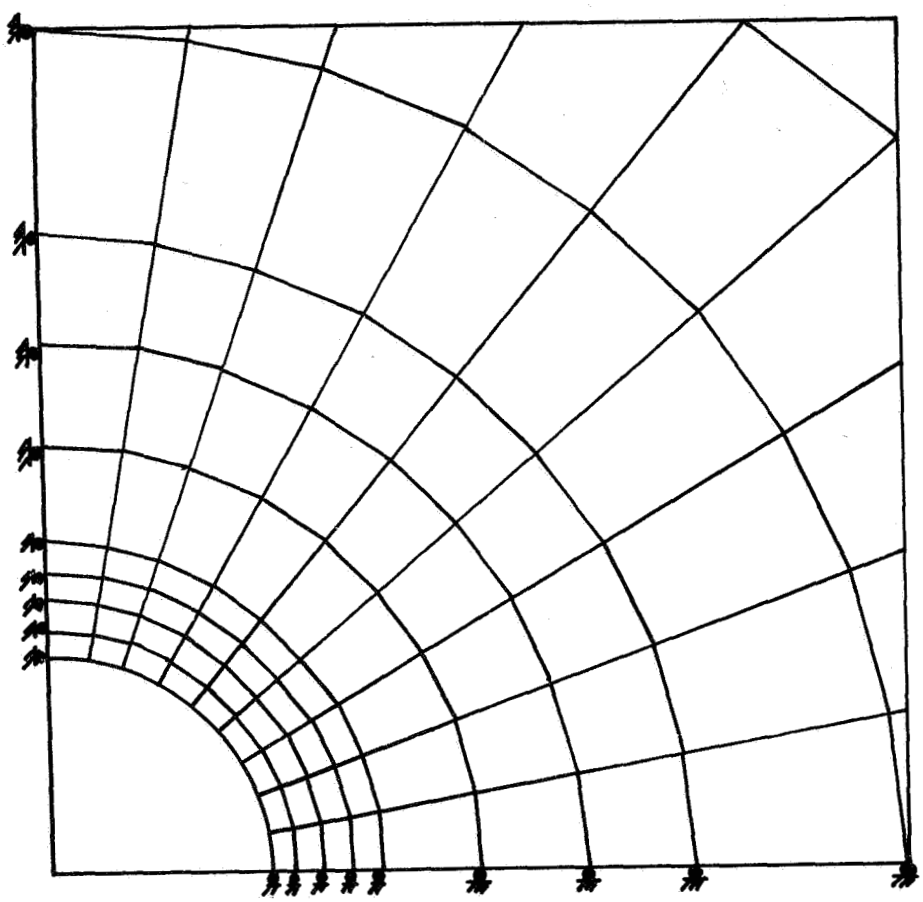

Figure 5.- Element assignment.